



Variable glacier response to atmospheric warming, northern Antarctic Peninsula, 1988–2009

B. J. Davies¹, J. L. Carrivick², N. F. Glasser¹, M. J. Hambrey¹, and J. L. Smellie³

¹Centre for Glaciology, Institute for Geography and Earth Sciences, Aberystwyth University, Llandinam Building, Penglais Campus, Aberystwyth SY23 3DB, UK

²School of Geography, University of Leeds, Leeds LS2 9JT, UK

³Department of Geology, University of Leicester, Leicester LE1 7RH, UK

Correspondence to: B. J. Davies (bdd@aber.ac.uk)

Received: 2 December 2011 – Published in The Cryosphere Discuss.: 21 December 2011

Revised: 11 July 2012 – Accepted: 23 August 2012 – Published: 21 September 2012

Abstract. The northern Antarctic Peninsula has recently exhibited ice-shelf disintegration, glacier recession and acceleration. However, the dynamic response of land-terminating, ice-shelf tributary and tidewater glaciers has not yet been quantified or assessed for variability, and there are sparse data for glacier classification, morphology, area, length or altitude. This paper firstly classifies the area, length, altitude, slope, aspect, geomorphology, type and hypsometry of 194 glaciers on Trinity Peninsula, Vega Island and James Ross Island in 2009 AD. Secondly, this paper documents glacier change 1988–2009. In 2009, the glaciated area was $8140 \pm 262 \text{ km}^2$. From 1988–2001, 90 % of glaciers receded, and from 2001–2009, 79 % receded. This equates to an area change of -4.4% for Trinity Peninsula eastern coast glaciers, -0.6% for western coast glaciers, and -35.0% for ice-shelf tributary glaciers from 1988–2001. Tidewater glaciers on the drier, cooler eastern Trinity Peninsula experienced fastest shrinkage from 1988–2001, with limited frontal change after 2001. Glaciers on the western Trinity Peninsula shrank less than those on the east. Land-terminating glaciers on James Ross Island shrank fastest in the period 1988–2001. This east-west difference is largely a result of orographic temperature and precipitation gradients across the Antarctic Peninsula, with warming temperatures affecting the precipitation-starved glaciers on the eastern coast more than on the western coast. Reduced shrinkage on the western Peninsula may be a result of higher snowfall, perhaps in conjunction with the fact that these glaciers are mostly grounded. Rates of area loss on the eastern side of Trinity Peninsula are slowing, which we attribute to the floating ice tongues

receding into the fjords and reaching a new dynamic equilibrium. The rapid shrinkage of tidewater glaciers on James Ross Island is likely to continue because of their low elevations and flat profiles. In contrast, the higher and steeper tide-water glaciers on the eastern Antarctic Peninsula will attain more stable frontal positions after low-lying ablation areas are removed, reaching equilibrium more quickly.

1 Introduction

The relatively small and dynamic northern Antarctic Peninsula Ice Sheet (Vaughan et al., 2003) is located in a region of particularly rapid atmospheric warming, with mean air temperature increasing by 2.5°C from 1950–2000 (Turner et al., 2005). The -9°C annual isotherm (the thermal limit of ice shelves determined from observational data) (Morris and Vaughan, 2003; Scambos et al., 2003) has moved southwards, resulting in $28\,000 \text{ km}^2$ being lost from Antarctic Peninsula ice shelves since 1960 (Cook and Vaughan, 2010). Ice-shelf tributary glaciers accelerated and thinned following the disintegration of part of the Larsen Ice Shelf (De Angelis and Skvarca, 2003), with up to a six-fold increase in centre-line speeds (Scambos et al., 2004). Other tidewater glaciers are accelerating, thinning and shrinking in response to increased atmospheric and sea surface temperatures (Pritchard and Vaughan, 2007). The present-day ice loss for the Antarctic Peninsula is -41.5 Gt yr^{-1} (Ivins et al., 2011), derived from Gravity Recovery and Climate Experiment (GRACE) measurements and GPS bedrock uplift data.

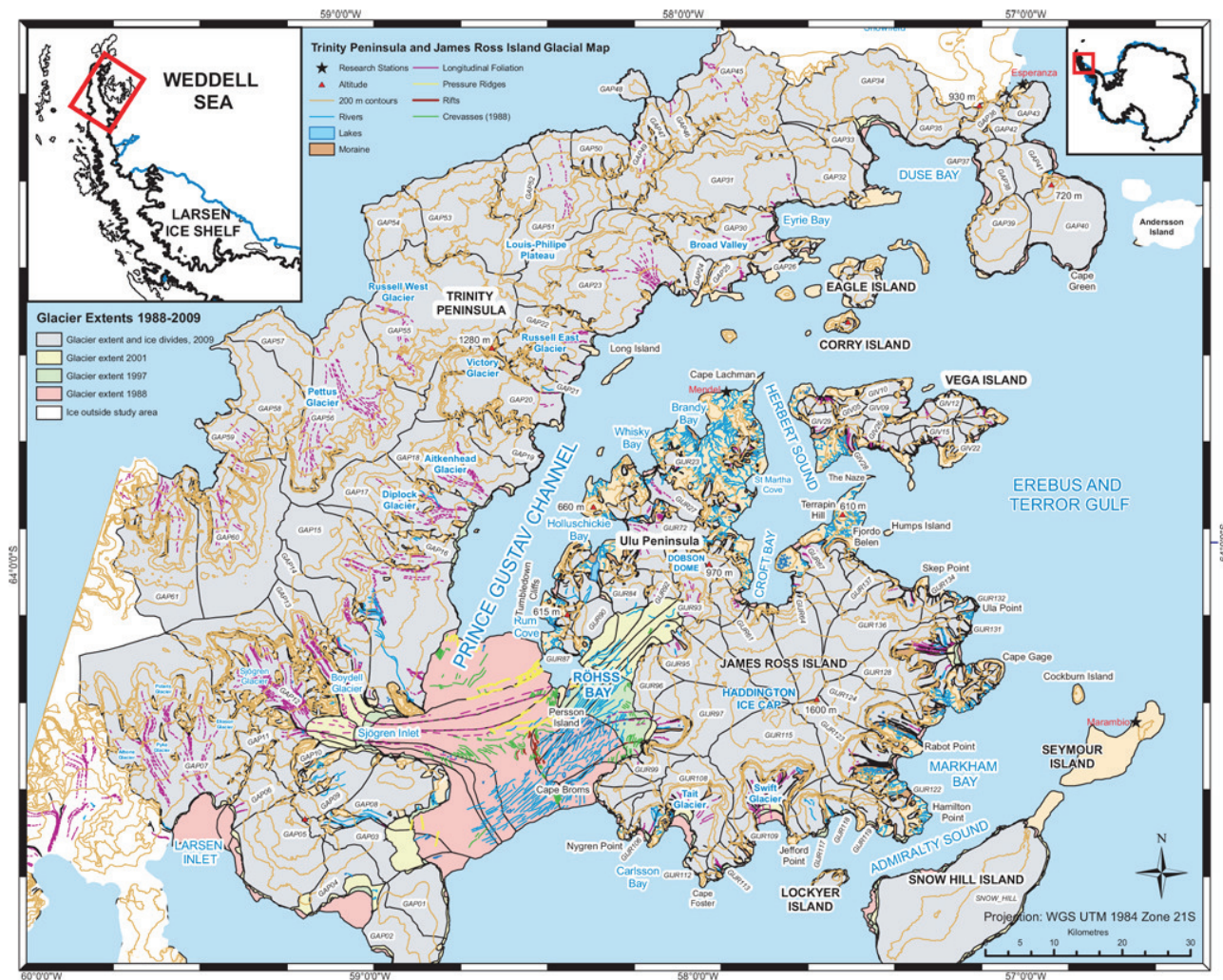


Fig. 1. Index map of the study region, showing ice divides, glacier drainage basins and glacier ID codes. Remotely sensed images (Table S1) used in making this map and all subsequent maps were projected in the Universal Transverse Mercator (UTM) projection World Geodetic System (WGS) 1984 Zone 21S.

Glacier inventory mapping is an essential prerequisite for regional mass balance studies and for modelling future glacier extents, but a detailed and up-to-date glacier inventory does not exist for the northern Antarctic Peninsula (Racoviteanu et al., 2009; Leclercq et al., 2011). Previous inventories have focused on changes up to 2001, and contain few quantitative data (Rabassa et al., 1982; Skvarca et al., 1995; Rau et al., 2004). There are outstanding questions regarding how the tributary glaciers on James Ross Island and northeast Antarctic Peninsula have changed since the 1995 disintegration of Prince Gustav Ice Shelf (PGIS) (cf. Rott et al., 1996; Glasser et al., 2011), and the likely future behaviour of these glaciers. The comparatively long time elapsed since that event offers an unusual opportunity to analyse the response of tidewater and ice-shelf tributary glaciers to ice shelf removal.

Therefore, the aim of this study was to create an inventory of the glaciers of Trinity Peninsula, James Ross Island and Vega Island (Fig. 1), and to analyse change in glacier extent from 1988–2009. There are five objectives: (i) to map the length and extent of each individual glacier in 1988, 1997, 2001 and 2009; (ii) to quantify glacier characteristics; (iii) to establish rates of recession for these glaciers from 1988 to 2009; (iv) to analyse spatial and temporal variability in recession rates, and (v) to determine controls upon recession rates.

2 Regional setting

2.1 Location and climate

The study region extends from Cape Dubouzet (63° S, 57° W) to Larsen Inlet (64° S, 59° W). James Ross Island

is separated from Trinity Peninsula by Prince Gustav Channel (Fig. 1). The Antarctic Peninsula mountains are an orographic barrier to persistent Southern Ocean westerlies. Cold continental air in the Weddell Sea also flows northwards, barring the warmer maritime air masses of the Bellingshausen Sea (King et al., 2003). The western Antarctic Peninsula, therefore, has a polar maritime climate, dominated by the relatively warm and ice-free Bellingshausen Sea, whilst the eastern Antarctic Peninsula and James Ross Island have a polar continental climate, dominated by the Weddell Sea, which is ice-bound for much of the year (Vaughan et al., 2003; King et al., 2003). At the same latitude in 2000 AD, mean annual air temperature on James Ross Island was -7°C , compared with -3°C on the western Peninsula (Morris and Vaughan, 2003).

Climate records from the South Orkney Islands suggest that regional warming probably began in the 1930s (Vaughan et al., 2003). The greatest warming rates are in the east (at Marambio and Esperanza stations; cf. Fig. 1), and the smallest on the northwest coast. The Antarctic Oscillation represents the periodic strengthening and weakening of the belt of tropospheric westerlies that surround Antarctica (van den Broeke and van Lipzig, 2004). A strengthening of this circumpolar vortex results in an asymmetric surface pattern change, with pressure falling over Marie Byrd Land. This pressure pattern causes northerly flow anomalies, which in turn produce cooling over East Antarctica and warming over the Antarctic Peninsula. Decreased sea ice in the Bellingshausen Sea enhances warming over the western Peninsula and the Weddell Sea. This is associated with decreases in precipitation over the south-western Peninsula (van den Broeke and van Lipzig, 2004; van Lipzig et al., 2004). Since the 1950s, the Antarctic Circumpolar Current at 60°S has warmed by 0.2°C , with the warming greatest near the surface (Gille, 2008), and waters to the west of the Antarctic Peninsula have warmed very rapidly (Turner et al., 2005; Mayewski et al., 2009).

2.2 Glaciology

Trinity Peninsula outlet glaciers, which attain altitudes of over 1600 m a.s.l., flow predominantly east and west, perpendicular to the Peninsula spine (Fig. 1). On the eastern flank many outlet glaciers terminate in floating or partly floating tongues. The north-western Trinity Peninsula coastline mainly comprises of grounded ice cliffs (Ferrigno et al., 2006).

In the late 1970s, 80 % of James Ross Island was ice-covered (Rabassa et al., 1982). The Mount Haddington Ice Cap drains over steep cliffs into outlet glaciers (Skvarca et al., 1995). The bedrock structure of resistant volcanic rocks overlying soft Cretaceous sediments (Smellie et al., 2008) fosters the development of elongate, over-deepened cirques, with steep or near vertical back walls up to 800 m high. Vega Island is dominated by two plateau ice caps that feed numer-

ous small tidewater glaciers. Snow Hill Island, Corry Island and Eagle Island (Fig. 1) bear marine-terminating ice caps.

Receding tidewater termini have been mapped for the entire Trinity Peninsula, with outlet glaciers on James Ross Island showing large reductions in area since the 1940s (Ferrigno et al., 2006). PGIS was connected to Larsen Ice Shelf until 1957/58 (Cook and Vaughan, 2010). The northernmost ice shelf on the eastern Antarctic Peninsula, it was the first to show signs of retreat (Ferrigno et al., 2006), and rapidly disintegrated in 1995 (Skvarca et al., 1995), followed by the thinning, acceleration and rapid recession of the former ice-shelf feeding glaciers (Rau et al., 2004; Glasser et al., 2011). An average shrinkage rate for James Ross Island glaciers of $1.8 \text{ km}^2 \text{ a}^{-1}$ from 1975–1988 (Skvarca et al., 1995) doubled after the disintegration of PGIS, to $3.8 \text{ km}^2 \text{ a}^{-1}$ between 1988 and 2001 (Rau et al., 2004).

3 Methods

3.1 Data sources

Our methods conform to those set out by the GLIMS programme (Racoviteanu et al., 2009). Mapping was conducted in ArcGIS 9.3 from interpretation of 2009 and 2001 ASTER images and Level 1G Landsat images from 1988 and 1990 (Tables 1 and S1; obtained from the USGS). The Antarctic Digital Database (ADD, <http://www.add.scar.org>) (from Cook et al., 2005) was used to provide additional data where the ice margin was difficult to map (e.g., because of high cloud cover), and for a limited number of glaciers in 1997. Topographic elevation data and contours were derived from the 2006 SPIRIT Digital Elevation Model (DEM) (Table 1). Ground-control points were not necessary because of the accurate geolocation of the SPOT-5 images (Reinartz et al., 2006; Korona et al., 2009). Glacier names and numbers were taken from previous glacier inventories and published maps (Rabassa et al., 1982; British Antarctic Survey, 2010). Holes in the DEM were filled using hydrological tools in the GIS. These holes were mostly on the flat plateaux of the peninsula, and the largest were 4 km in diameter. This reduced errors introduced by clouds and poor image correlation in areas with a lack of topographic features. However, because the holes were in areas of generally flat plateaux, the uncertainties that this introduced into the study were minimised.

3.2 Glacier and drainage basin delineation

Glacier polygons for the year 2009 were manually digitised. Possible uncertainties include misclassification of snow and ice, delineation of debris-covered glaciers and digitisation errors. Ice divides were determined through analysis of the SPIRIT DEM (identifying cols, high points and breaks in slope, using models of aspect and slope (Fig. S1, Table S2; Svoboda and Paul, 2009; Bolch et al., 2010), and using hydrological tools in ArcToolbox to determine surface flow and

Table 1. Data sources used in Trinity Peninsula glacier inventory.

| Data Source | Resolution | Swath | Date Captured | Notes |
|---|---|--------|--|--|
| ASTER VNIR (Advanced Spaceborne Thermal Emission and Reflection Radiometer) | 15 m | 60 km | Various from 2001 to 2009* | Sensor on the NASA Terra Satellite. Level 1B Multispectral images. |
| Landsat-4 TM | 28.5 m | 185 km | 29 February 1988, 9 February 1990 | Scene ID: LT4215105160XXX11 Scene ID: LT42161051990040XXX01 |
| SPOT-5 (Satellite Pour l'Observation de la Terre) HRS (High Resolution Sensor) orthoimages | 5 m, absolute horizontal precision of 30 m RMS. | 120 km | AP: 7 January 2006 JRI: 23 January 2006 | Panchromatic. AP: Incidence angle of -22.8° , sun azimuth of 55.2° and sun elevation of 40.5° . JRI: Incidence angle of -22° , sun azimuth of 55° and sun elevation of 37° . |
| SPIRIT DEM V1 (SPOT-5 Stereoscopic Survey of Polar Ice: Reference Images and Topographies) | 40 m. Vertical precision ± 6 m | 185 km | Dates as above for the two DEMs | Derived from the above SPOT-5 HRS stereoscopic pairs. |

*Refer to Supplementary Methods for further details of ASTER images.

drainage basins), and through glaciological mapping. Glaciological structures were identified on the 2009 ASTER and 2006 SPOT-5 images (Fig. S1; Table S1) according to previously published criteria (Glasser et al., 2009, 2011). The availability of multi-temporal images (Table S1) aided the identification of perennial snow (noted in *Remarks* attribute). Glaciers less than 0.1 km^2 were excluded from this study because of difficulties in identification, accurate mapping and the danger of misclassification of snow patches.

The largest uncertainties in glacier drainage basin delineation are derived from interpreter error of ice-divide identification and mapping (Table 2), which is also limited by DEM quality in areas of flat white ice. ASTER Level 1B images are pre-processed, but were co-registered to the SPOT-5 images to reduce uncertainties. Mapping was estimated to be accurate to within 3 pixels (i.e., 45 m). A buffer of 22.5 m width was, therefore, placed on either side of each glacier polygon, providing a minimum and maximum estimate of size. Assuming no migration of ice divides, this produces an unnecessarily large absolute error for each subsequent year of analysis. Therefore, we also used a 3-pixel wide buffer only around the frontal margin of the glacier in order to capture errors in mapping the change in glacier snout position. Cumulative uncertainties are estimated by calculating the square-root of the sum of the squares. The uncertainty is likely to be at the upper bound.

The extent and length of each glacier was also mapped for 1988, 1997 and 2001. In subsequent analyses, glacier surface areas that changed less than the uncertainty were classified as “stationary”. “Shrinkage” indicates a loss of surface area, while “recession” indicates a reduction in glacier length.

3.3 Attribute data for glacier drainage basins

Attribute information for each glacier polygon comprises standard GLIMS data, including *Area*, *Length*, *Coordinates*, *Name* (if published), *Glacier ID* (e.g., GAP17 or GIJR65, standing for Glacier Antarctic Peninsula and Glacier James Ross Island, respectively; these conform where appropriate to previous inventories), *GLIMSID*, *Elevation*, *Width of calving front*, *Date of scene acquisition*, *Satellite*, *Tongue*, *Primary classification*, *Form*, *Frontal characteristics*, *Moraines*, *Debris on tongue*, *Remarks*, *Slope*, *Aspect*, *Equilibrium Line Altitude (ELA)* and *Hypsometry*, in addition to notes on geomorphology and glaciology (cf. Rau et al., 2005; Raup et al., 2007a,b; Racoviteanu et al., 2009; Paul et al., 2010; Raup and Khalsa, 2010).

Glacier *Length* was measured along the centre-line profile (cf. Lopez et al., 2010), following the steepest downward gradient and, where possible, along surface-flow trajectories. In glaciers with multiple cirques and accumulation areas, *Length* was measured according to the longest distance. Ice caps and ice fields were not measured.

Data were automatically derived in the GIS for minimum (H_{MIN}), maximum (H_{MAX}), mean (H_{MEAN}) and median (H_{MEDIAN}) elevation using the 2006 SPIRIT DEM. Aspect (or glacier orientation) is required for statistical modelling of glaciers (Paul et al., 2010; Evans, 2006). Mean slope can be used as a proxy for ice thickness (Haeberli and Hoelzle, 1995; Paul et al., 2010). Mean values were derived through decomposition with the sine and cosine values of the SPIRIT DEM (Paul et al., 2010) (Table S2).

Table 2. Sources of uncertainty and mitigation in defining the area of each glacier polygon.

| Sources of uncertainties | Uncertainty | Mitigation |
|--|--------------------------|--|
| Ice-divide and drainage basin identification | ±10 % | Multiple methods used for ice-divide identification (DEM, visual, glaciological interpretations, slope, aspect, automatic hydrology tools). |
| Identification of glacier boundaries (digital mapping uncertainty) on ASTER images | 3 pixels (± 22.5 m) | Visual checks and buffer width of 22.5 m on either side of glacier polygon |
| Identification of glacier boundaries (digital mapping uncertainty) on Landsat-4 TM image | 3 pixels (± 112.5) | Visual checks and buffer width of 112.5 m on either side of glacier polygon |
| Delineation of debris-covered tongues | ±0.5 % | Visual checks and buffer width (as above); checking over several images where possible |
| Scene quality, clouds, seasonal snow, shadows | ±4 % | Snow coverage of glacier margins is covered in the <i>Remarks</i> column of the database. Use of multiple images aids the omission of seasonal snow. |
| Uncertainty in co-registration and glacier size | ±15 m (RMS) for VNIR | Error is less than 3 pixels so is included in the buffer above |

In the *Tongue* parameter, glaciers were categorised as floating, partially floating, grounded or land-terminating. Floating tongues typically have a pronounced break in slope at the grounding-line, an irregular heavily crevassed and convex calving front, a flat long profile, an irregular margin, and occasional large rifts. Grounded tidewater glaciers are typically characterised by a concave calving front, a steadily dipping long profile, and have no clear break in slope (Scambos et al., 2004; Reinartz et al., 2006; Lambrecht et al., 2007; Fricker et al., 2009).

Glacier hypsometric curves were calculated by masking glacier polygons with the 40×40 m resolution SPIRIT DEM (see Paul et al., 2010). This parameter was only applied to glaciers over 40 km^2 , and normalised hypsometric curves were, therefore, created for 54 of the 194 glaciers. A single Hypsometric Index (HI) was calculated for each glacier polygon using the Eq. (1) below, originally presented by Jiskoot et al. 2009, where:

$$\text{HI} = \frac{H_{\text{median}} - H_{\max}}{H_{\text{median}} - H_{\min}}, \text{ and if } 0 < \text{HI} < 1, \quad (1)$$

$$\text{then } \text{HI} = \frac{-1}{\text{HI}}$$

This gives a single index of glacier hypsometry for each glacier and allows them to be grouped into one of five categories (cf. Jiskoot et al., 2009).

3.4 Equilibrium line altitude derivation

In this study, five different long-term ELA derivation methods were applied (Table 3). Median Elevation (H_{MEDIAN})

correlates well with the balanced-budget ELA (Braithwaite and Raper, 2009; Paul and Svoboda, 2009). ELA_{AAR} assumed an AAR of 0.6, which is typical of steady-state conditions (Torsnes et al., 1993). However, ELA_{AAR} may be ineffective on marine-terminating glaciers (Leonard and Fountain, 2003). Toe to Headwall Ratio (ELATHAR) has been used on small Alpine and Norwegian glaciers, and uses the ratio between the minimum and maximum altitude of the glacier (Torsnes et al., 1993; Carrivick and Brewer, 2004).

The “Hess” method is determined from the transition of convex to concave contours (Leonard and Fountain, 2003; Jiskoot et al., 2009). This method is difficult to apply in glaciers that are marine-terminating, have steep ice falls or complex or compound cirques (Jiskoot et al., 2009).

Mapping the snow line (firn line) at the end of the ablation season over several years may be a proxy for the long-term average ELA (Jiskoot et al., 2009; Braithwaite and Raper, 2009). However, this method could not be used due to cloud or unsuitable snow cover on glaciers on the available scenes. Finally, the strong east-west precipitation gradient on Trinity Peninsula results in snow lines close to sea level on the western coast, and snow lines at 300 to 400 m a.s.l. on the eastern Peninsula. Strong winds also affect the distribution of snow at the end of the ablation season.

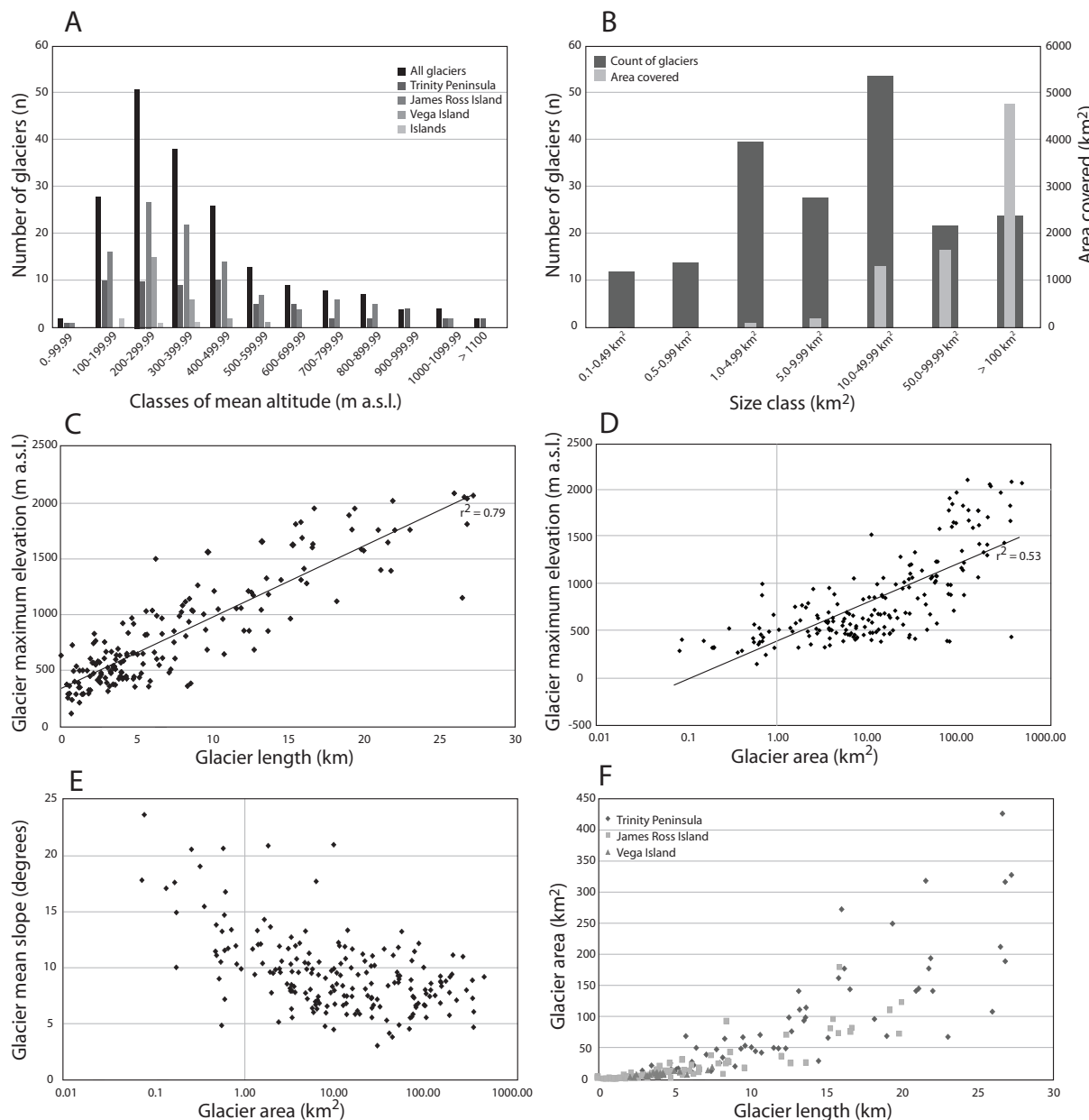


Fig. 2. Glacier inventory data. See Table 5 for p-values. **(A)** Mean elevation of glaciers in each region. **(B)** Frequency distribution of different glacier area classes, compared with total area in each size class. **(C)** Glacier maximum elevation and length. **(D)** Maximum elevation and area. **(E)** Mean slope and log glacier area. **(F)** Glacier area and length.

4 2009 Glacier inventory results

4.1 Glacier size, elevation, and classification

In 2009, the northern Antarctic Peninsula region had 194 glaciers covering $8140 \pm 262 \text{ km}^2$ (Fig. 1; Table 4). The mean elevation of glaciers was skewed towards glaciers in the 200–300 m a.s.l. bin (Fig. 2a). A small number of glaciers over 100 km^2 account for most of the glacierised area (Fig. 2b). As the total area of glaciers in the size class 0.1–0.5 km^2 is only

3 km^2 , the underestimate of glacierised area caused by having a minimum glacier size of 0.1 km^2 is likely to be insignificant and certainly considerably less than 3 km^2 . H_{MEAN} of glaciers on Trinity Peninsula peaked at 400 m a.s.l., reflecting its high mountain chain. James Ross Island had the highest number of glaciers with mean elevations above 200 m.

The relationship between glacier elevation, length, area and slope was investigated, as these parameters may control glacier recession and behaviour. There was a strong correlation between glacier length and maximum elevation

Table 3. Methods of ELA calculation. Refer to the Supplementary Methods for more information. Altitudes are derived from the 2006 SPIRIT DEM, and these ELAs are, therefore, approximations for the year 2006.

| Method | Description | Notes |
|-----------|-------------------------|---|
| ELAMEDIAN | Median Elevation | Represents an accumulation area ratio (AAR) of 50 %. Equivalent to H_{MEDIAN} . Applied to all glaciers. |
| ELAAAR | Accumulation Area Ratio | Assumes an AAR of 60 %; derived from hypsometric curves for the 54 tidewater glaciers over 40 km ² . Applied to 54 glaciers. |
| ELATHAR | Toe to Headwall Ratio | Ratio between minimum and maximum glacier altitude. Applied to all glaciers. |
| ELAHESS | Hess method | Transition between convex and concave contours. Applied to 69 glaciers, of which only 13 are land-terminating. |
| ELAMEAN | Mean ELA | Mean of ELAMEDIAN, ELAAAR, ELATHAR |

Table 4. Summary table of the glaciers of the northern Antarctic Peninsula. Uncertainty is determined by applying a 22.5 m buffer to either side of the glacier polygon. TP=Trinity Peninsula. JRI=James Ross Island. VI=Vega Island. IIC=Island Ice Caps.

| | Number of Glaciers | Total glacierised area (km ²) | Total land area (km ²) | % Glacierised |
|-------|--------------------|---|------------------------------------|---------------|
| TP | 62 | 5827 ± 154 | 6160 | 95 |
| JRI | 104 | 1781 ± 86 | 2378 | 75 |
| VI | 24 | 168 ± 15 | 253 | 66 |
| IIC | 4 | 365 ± 7 | 407 | 90 |
| Total | 194 | 8140 ± 262 | 9198 | 89 |

($r^2 = 0.8$; Fig. 2c), and a rather weaker correlation between log glacier area and elevation ($r^2 = 0.5$; Fig. 2d; Table 3). There is a weak relationship with log glacier area, H_{MEAN} , slope and length (Figs. S2, 2e, f) and between glacier length and slope (Table 5). Length and mean slope may not be correlated because of the unusual shape of the glaciers on James Ross Island, with flat upper and lower portions, separated by steep ice falls.

Outlet or valley glaciers drain the large plateau ice caps that rest on the Trinity Peninsula mountain chain (Table 6). Of these glaciers, 10 had floating and 20 had partially floating termini. James Ross Island had 16 glaciers with floating termini (Fig. 3a) and one lacustrine glacier (GIJR86). James Ross Island also had 17 out of the 18 small alpine glaciers.

4.2 Equilibrium line altitudes

There is a very strong correlation between ELAMEDIAN, ELAAAR and ELATHAR (Fig. S2; Table 5). H_{HESS} was not used as it produced large scatter and was only applicable to a small number of glaciers. ELAMEAN is, therefore, the average of ELAMEDIAN, ELAAAR and ELATHAR. However, the calculated ELAMEAN for each glacier must be treated neces-

sarily with caution, as it is entirely derived from the altitudinal range and hypsometric curves of the glaciers, has not been checked against mass-balance data, and does not take into account east-west orographic precipitation and wind variations. Uncertainties range from < 5 m to > 500 m, illustrating the difficulty in obtaining a meaningful parameter from topographical data alone. Finally, ELAs are ideally measured on glaciers that are in a balanced state. Our study has shown that almost all the glaciers analysed are shrinking and are, therefore, in a state of negative mass balance. In addition, estimating the ELA of polar tidewater glaciers is difficult, because their mass flux is controlled by calving processes.

Figure 3b shows the distribution of ELA over the study region. The subdued topography on Ulu Peninsula, James Ross Island, results in low ELAMEAN of around 100 m a.s.l. However, the glaciers that have accumulation areas on the Mount Haddington Ice Cap can have ELAMEAN > 800 m a.s.l. ELAMEAN on Trinity Peninsula are generally around 500 to 600 m a.s.l., with the exception of GAP60 and 61, which have ELAMEAN of 1194 ± 727 and 1265 ± 787 m a.s.l., respectively. The large range of values is less for land-terminating

Table 5. Regression table for variables in the inventory. n is the number of observations. “ltg” means “land-terminating glacier”. P-values are calculated at the 95 % confidence level.

| Variable A | Variable B | n | Adjusted r^2 | Standard error | P-value |
|-------------------------|-----------------------|-----|----------------|----------------|---------|
| Maximum Elevation | Glacier length | 174 | 0.79 | 3.10 | < 0.001 |
| Maximum Elevation | Glacier area | 192 | 0.48 | 51.22 | < 0.001 |
| Mean Elevation | Glacier area | 192 | 0.30 | 59.57 | < 0.001 |
| Mean Slope | Glacier area | 192 | 0.05 | 69.38 | 0.001 |
| Mean Slope | Glacier length | 174 | 0.08 | 3.14 | < 0.001 |
| Mean Aspect | Mean Elevation | 192 | 0.02 | 235.84 | 0.160 |
| Mean Aspect | Maximum Elevation | 192 | 0.00 | 106.81 | 0.814 |
| ELA _{MEDIAN} | ELA _{AAR} | 55 | 0.95 | 72.21 | < 0.001 |
| ELA _{MEDIAN} | ELA _{THAR} | 192 | 0.62 | 159.30 | < 0.001 |
| 1988 glacier area (ltg) | Total area lost (ltg) | 55 | 0.19 | 3.24 | < 0.001 |
| ELA _{MEAN} | Total area lost | 186 | 0.04 | 200.10 | 0.003 |
| Maximum Elevation | Total area lost | 186 | 0.14 | 428.78 | < 0.001 |

Table 6. Summary of glacier descriptors. All = all glaciers.

| | TP | JRI | VI | IIC | All |
|------------------------|-------------------------|-----|----|-----|-----|
| Primary Classification | Ice Cap | 11 | 18 | 13 | 4 |
| | Ice Field | 1 | 0 | 0 | 0 |
| | Outlet glacier | 27 | 45 | 11 | 0 |
| | Valley Glacier | 21 | 16 | 0 | 0 |
| | Mountain Glacier | 1 | 17 | 0 | 0 |
| | Glacieret and snowfield | 1 | 8 | 0 | 0 |
| | | | | | 9 |

simple-basin glaciers. For example, GIJR103, a grounded valley glacier with a simple basin, has an ELAMEAN of 87 ± 1 m a.s.l. The range of uncertainties for simple basin glaciers with floating tongues (such as, for example, GIJR64, ELAMEAN 909 ± 432 m a.s.l.) are due to their large low-lying ablation areas.

4.3 Glacier aspect

Flow on Trinity Peninsula is generally perpendicular to, and away from, the central spine (Fig. 3c and e). There is no correlation between aspect and elevation (Fig. 2i; Table 5). Most glaciers display asymmetry over their surface area, which results in a strong northeast to west-facing preferred glacier aspect on Trinity Peninsula (Fig. 3c). On James Ross Island, there is a preference for northwest-facing aspects. Aspects on Vega Island trend largely southeast and northwest.

4.4 Glacier hypsometry

The hypsometric index (HI) of all glaciers was calculated and glaciers were divided into five categories (Fig. 3d; Jiskoot et al., 2009). There was considerable inter-catchment variability in glacier shape and elevation distributions. Over half (35) of the large outlet glaciers on Trinity Peninsula were very bottom-heavy, with large low-lying areas below the median altitude (Figs. 3d, f). Exceptions are a few glaciers that termi-

nate within narrow bays (e.g., GAP13, GAP17). However, on the west coast of Trinity Peninsula, glaciers are more equidimensional or top-heavy. Glaciers that were formerly tributaries to PGIS were large with relatively small accumulation areas. The remaining glaciers on eastern Trinity Peninsula were generally bottom-heavy, for example, GAP34, GAP31 and GAP20.

On James Ross Island, the low-lying topography of Ulu Peninsula resulted in bottom-heavy outlet glaciers draining Dobson Dome (Fig. 3d, f), but the large Mount Haddington Ice Cap contained largely top-heavy glaciers, such as GIJR115 and GIJR61. The long-profiles of tidewater outlet glaciers draining the Mount Haddington Ice Cap are typified by large, flat accumulation areas with sharp changes in slope angle at their cirque headwalls, followed by large, low-lying and relatively flat (partly) floating tongues (Fig. 3g).

In Fig. 4, examples of normalised hypsometric curves derived from the 2006 SPIRIT DEM are presented, illustrating the difference between bottom-heavy, equi-dimensional and top-heavy glaciers. Comparing the hypsometric curves in Fig. 4 with the long profiles presented in Fig. 3g, it is obvious that the Mount Haddington Ice Cap outlet glaciers have large, low-lying ablation areas and relatively flat, low-angled accumulation areas.

5 Glacier change results

5.1 Change in glacierised area

On Fig. 1, the extent of glaciers in 1988, 1997, 2001 and 2009 is shown. The total area given is a minimum value. There was only satellite coverage of all three years (1988, 2001 and 2009) for 178 glaciers. Data for 1997 is particularly limited. 90 % of glaciers receded in the period 1988–2001, and 79 % shrank from 2001–2009 (Table 7). On Trinity Peninsula and Vega Islands, small advances only occurred from 1988–2001

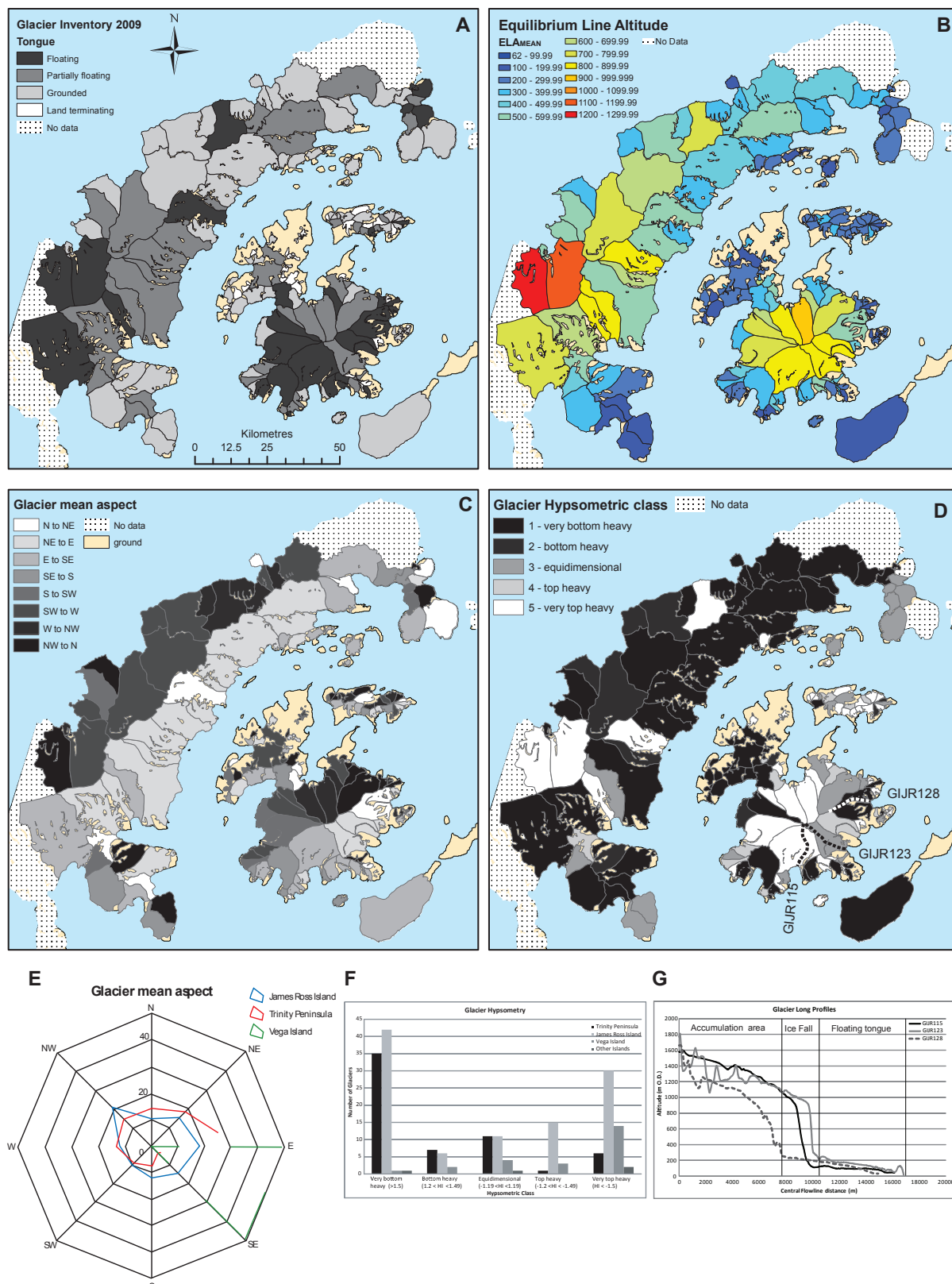


Fig. 3. (A) Floating, partially floating and grounded tongues at glacier termini in 2009. (B) Mean ELA in 2006. (C) Mean aspect in 2006. (D) Distribution of hypsometric classes. (E) Percentages of glaciers in each cardinal direction. (F) Frequency distribution of different hypsometric indices in different regions. (G) Long profiles of three tidewater glaciers on James Ross Island in 2006.

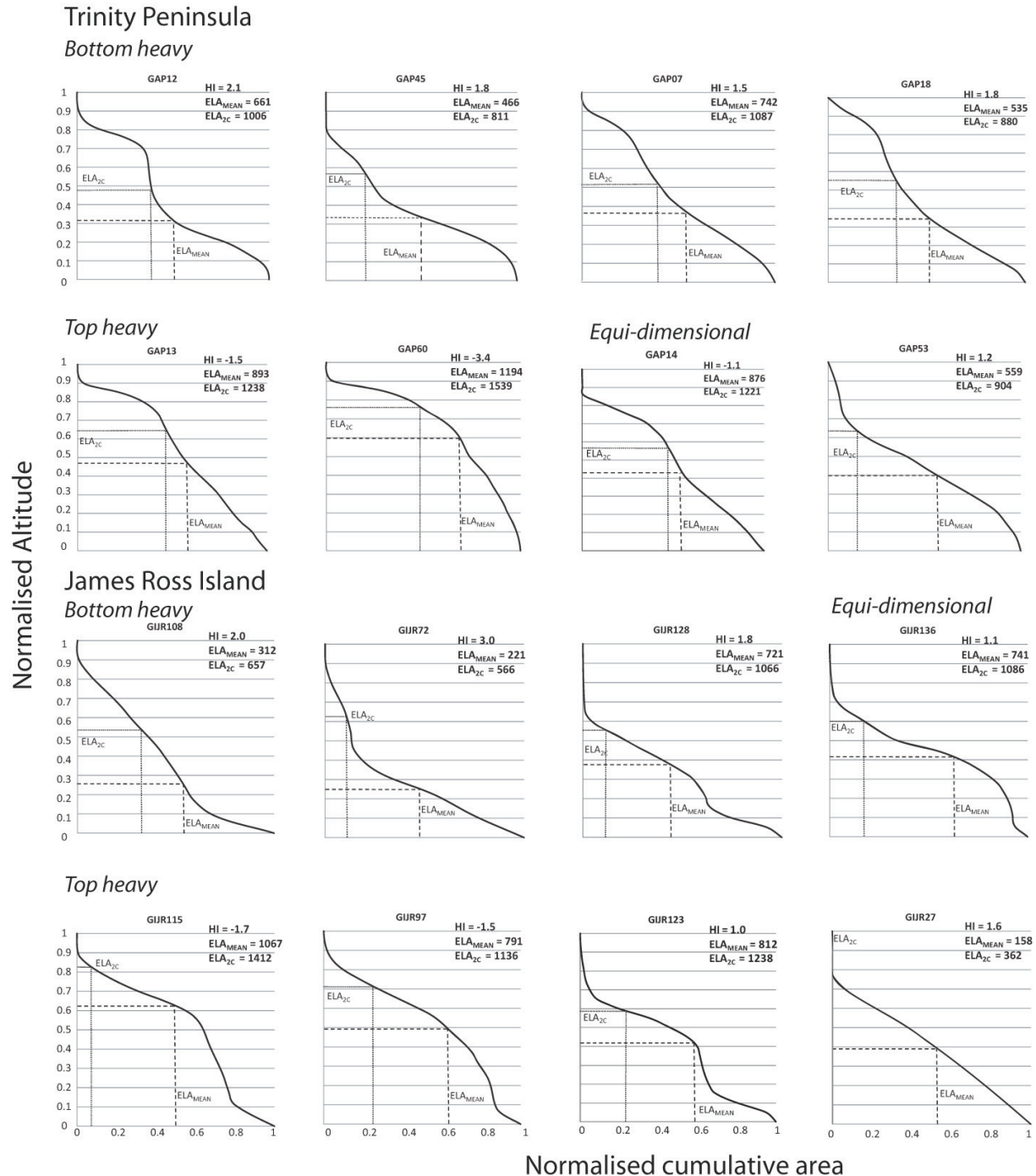


Fig. 4. Normalised hypsometric curves of representative tidewater glaciers on Trinity Peninsula and James Ross Island. Normalised ELA_{MEAN} for each glacier is plotted. ELA_{2C} indicates the possible change in equilibrium line with future climate change. A 2 °C warming could result (presuming an adiabatic lapse rate of $-5.8^{\circ}\text{C}/1000\text{ m}$) in a rise in ELA of 345 m.

in two glaciers. On James Ross Island, three glaciers advanced from 1988–2001 (Tables 7 and 8). It is noteworthy that different glaciers advanced in each time period, and that the number of advancing glaciers has decreased since 2001.

Most of the advancing glaciers were marine-terminating outlet glaciers.

The Trinity Peninsula glaciers cover $5827.3 \pm 153.9\text{ km}^2$, and from 1988–2001, lost 727.8 km^2 , equivalent to an average recession rate of $56\text{ km}^2\text{ a}^{-1}$. These glaciers then shrank

Table 7. Number of glaciers advancing and retreating in the period 1988 to 2009. Note that missing data means not all 194 glaciers were included

| | | Number of Glaciers | | | |
|-------------------|------------|--------------------|-------|-----------|------|
| | | 1988–2001 | | 2001–2009 | |
| | | No. | % | No. | % |
| All glaciers | Retreating | 160 | 89.9 | 146 | 79.3 |
| | Advancing | 8 | 4.5 | 3 | 1.6 |
| | Stationary | 9 | 5.6 | 35 | 19.0 |
| | Total | 178 | 100 | 184 | 100 |
| Trinity Peninsula | Retreating | 51 | 91.1 | 52 | 86.7 |
| | Advancing | 4 | 7.1 | 0 | 0 |
| | Stationary | 1 | 1.8 | 8 | 13.3 |
| | Total | 56 | 100 | 60 | 100 |
| James Ross Island | Retreating | 91 | 91.0 | 76 | 73.8 |
| | Advancing | 3 | 3.0 | 3 | 2.9 |
| | Stationary | 6 | 6.0 | 24 | 23.3 |
| | Total | 100 | 100 | 103 | 100 |
| Vega Island | Retreating | 14 | 82.4 | 15 | 88.2 |
| | Advancing | 1 | 5.9 | 0 | 0.0 |
| | Stationary | 2 | 11.8 | 2 | 11.8 |
| | Total | 17 | 100 | 17 | 100 |
| Island Ice Caps | Retreating | 4 | 100.0 | 3 | 75.0 |
| | Advancing | 0 | 0 | 0 | 0 |
| | Stationary | 0 | 0 | 1 | 25.0 |

at a rate of $16.8 \text{ km}^2 \text{ a}^{-1}$ in the 8 yr from 2001–2009. The glaciers on James Ross Island lost $290 \pm 15.2 \text{ km}^2$ of surface area between 1988 and 2001, and $121.9 \pm 15.2 \text{ km}^2$ between 2001 and 2009 (Table 8). This equates to an overall rate of areal loss on James Ross Island of $22.3 \text{ km}^2 \text{ a}^{-1}$ over the 13 yr from 1988–2001, and $15.1 \text{ km}^2 \text{ a}^{-1}$ over the 8 yr from 2001–2009. The majority of the area lost on James Ross Island is accounted for by the disintegration of PGIS in 1995. For most glaciers, the annual rate of retreat has accelerated since 2001, with those on eastern Antarctic Peninsula and James Ross Island exhibiting particularly rapid recession.

5.2 Land-terminating glaciers

The variability of land-terminating glaciers is of particular interest because their activity is directly related to climatic changes and these glaciers are scarce on the Antarctic Peninsula (Skvarca and De Angelis, 2003). In the study region, most are less than 1 km^2 , and so would be expected to react fastest to external forcings, although this can vary regionally (Raper and Braithwaite, 2009) and by elevation. Response times are also determined by slope and mass balance gradient (Oerlemans, 2005); Fig. 2e illustrates that there is a weak negative relationship between glacier area and mean slope (p -value of 0.001).

The seven land-terminating glaciers on Vega Island all lost area between 1988–2001 (Figs. 5a and b), with little shrinkage thereafter. Change in glacier area is between -2 to -7% . However, the land-terminating part of GIV09, which corresponds with Glaciar Bahía del Diablo in previous studies, remained stationary from 1988–2009, which agrees with previous workers (Skvarca et al., 2004). On James Ross Island, for glaciers $< 1 \text{ km}^2$, the percentage shrinkage varies from 0 to 66 % (Figs 5c, d). Glaciers $< 3 \text{ km}^2$ also show highly variable patterns of shrinkage, from 0 to 35 % (Figs. 5e, f). There is a weak correlation between initial glacier size (1988) and total glacier area lost (1988–2009; $r^2 = 0.19$; Fig. 5g; Table 5). This weak correlation is most easily explained by assuming that the glaciers have yet to reach a steady state.

The largest areal changes were observed in the period 1988–2001 (Fig. 5h). This supports initial observations by Rau et al. 2004. Of the 48 land-terminating glaciers we mapped on the island, 36 out of the 48 shrank from 1988–2001, and 15 shrank from 2001–2009.

5.3 Marine-terminating glaciers

Recession was greatest for ice-shelf tributary glaciers (Fig. 6a, b), with the fastest rates of length change in Sjögren Inlet from 1988–2001. For example, Sjögren Glacier (GAP12) receded 33 km from 1988 to 2001 and 7.1 km from 2001 to 2009, with a reduction in rate of change after 2001. Most of this change is related to the collapse of Prince Gustav Ice Shelf. Length changes for non-ice-shelf tributary glaciers on Trinity Peninsula are small by comparison, but they suffered faster annual rates of recession after 2001, with glaciers on eastern Trinity Peninsula receding more than glaciers on western Trinity Peninsula, many of which showed no change in length (Fig. 6a). Rates of recession were fastest for ice-shelf tributary glaciers, then for east-coast tidewater glaciers and slowest for west-coast glaciers.

In total, glaciers shrank by $1319.5 \pm 395.6 \text{ km}^2$ between 1988 and 2009. Of this areal decline, 70 % ($927.7 \pm 395.6 \text{ km}^2$) occurred prior to 1997 with the disintegration of PGIS in 1995 (Table 8). However, glacier shrinkage has continued, with $274 \pm 49.1 \text{ km}^2$ lost since 2001; this is equivalent to a total rate of areal loss of $30.4 \pm 1.0 \text{ km}^2 \text{ a}^{-1}$ since 2001.

6 Discussion

6.1 Spatial and temporal patterns of glacier change

On Trinity Peninsula, east-coast glaciers shrank at $0.35 \% \text{ a}^{-1}$ from 1988–2001, while west-coast glaciers shrank at $0.02 \% \text{ a}^{-1}$ (an insignificant amount) and ice-shelf tributary glaciers at $2.69 \% \text{ a}^{-1}$. From 2001–2009, east-coast tidewater glaciers shrank at $0.21 \% \text{ a}^{-1}$, west-coast glaciers at $0.03 \% \text{ a}^{-1}$, and ice-shelf tributary glaciers at $0.96 \% \text{ a}^{-1}$. Regional spatial differences in glacier recession on eastern and western Trinity Peninsula may be attributed

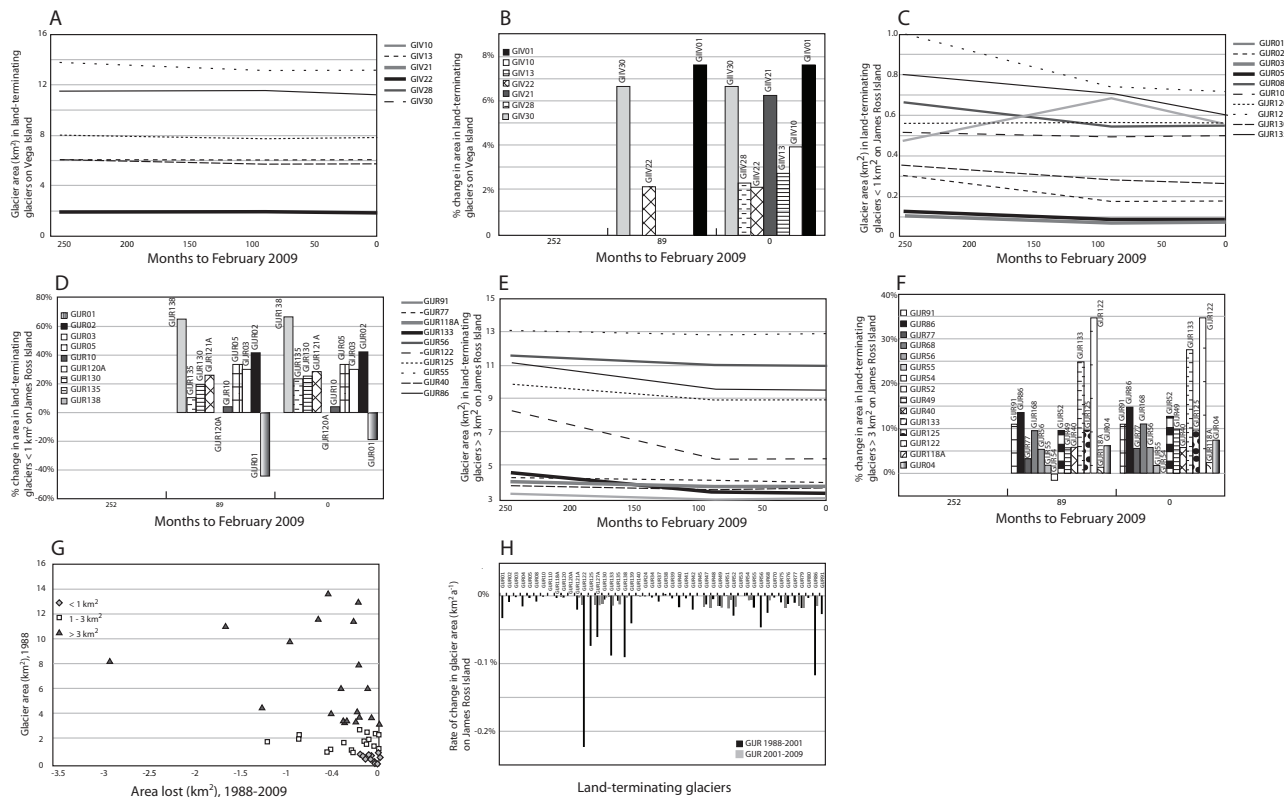


Fig. 5. Change in land-terminating glaciers on Vega Island and James Ross Island. **(A)** Percentage change in surface area on Vega Island. **(B)** Glacier shrinkage on Vega Island. **(C)** Percentage change for glaciers (less than 1 km^2) on James Ross Island. **(D)** Glacier change for small ($< 1 \text{ km}^2$) land-terminating glaciers on James Ross Island. **(E)** Percentage change for glaciers ($> 3 \text{ km}^2$) on James Ross Island. **(F)** Glacier change for glaciers ($> 3 \text{ km}^2$) on James Ross Island. **(G)** Change in glacier area and initial glacier size ($r^2 = 0.11$; see Table 5). **(H)** Variance in rates of change on James Ross Island.

to precipitation and temperature gradients, with the more stable western Trinity Peninsula receiving more snow (cf. van Lipzig et al., 2004; Aristarain et al., 1987; Vaughan et al., 2003).

Ice-shelf tributary glaciers shrank fastest overall and particularly rapidly from 1988–2001 (Fig. 7). Regions of exceptionally rapid glacier area loss on Trinity Peninsula include Larsen Inlet, Sjögren Inlet, Eyrie Bay and Duse Bay. The glaciers of Röhss Bay experienced enhanced drawdown and faster rates of annual recession after 2001. GIJR90 declined in area at a rate of $1.9 \text{ km}^2 \text{ a}^{-1}$ from 2001–2009, when the ice shelf retreated beyond the narrow pinning point at the head of Röhss Bay, but the margin was stationary from 1988–2001. These tidewater glaciers now no longer terminate in a discernible ice shelf, but calve directly into Röhss Bay.

Many large tidewater glaciers on James Ross Island suffered rapid areal decline from 1988 to 2009 (e.g., GIJR108 [$0.6 \text{ km}^2 \text{ a}^{-1}$] Fig. 1). There is strongly asynchronous behaviour (Fig. 7a). The glaciers of Croft Bay and GIJR72 [$0.1 \text{ km}^2 \text{ a}^{-1}$], in Holluschickie Bay, for example, declined comparatively little. Variable rates of areal shrinkage are also noticeable around Cape Broms of southeast James Ross Is-

land. In general, most glaciers shrank faster from 1988–2001, with some exceptions around Röhss Bay on James Ross Island, Snow Hill Island and the western Trinity Peninsula (Fig. 7, Table 7).

The observed asymmetry and variability in recession in tidewater glaciers may be explained by complex calving processes and nonlinear responses to changes in oceanic temperatures as well as atmospheric temperature and precipitation gradients. Ocean temperatures around the western Antarctic Peninsula have risen by more than 1°C since 1951 (Meredith and King, 2005), driven by reduced sea-ice formation and atmospheric warming. Changes in sea-surface temperatures (and sea ice extent) may influence enhance bottom melting and thinning (Holland et al., 2010) and, therefore, propensity to calve (Benn et al., 2007), thus, accelerating terminus retreat. Tensile strength of glacier ice decreases as ice becomes more temperate, resulting in increased calving rates (Powell, 1991). In grounded tidewater glaciers, terminus position may be controlled by the local geometry of the fjord (van der Veen, 2002). Furthermore, retreat of the terminus, as a result of increased calving, leads to larger up-glacier stretching rates, greater ice speeds and glacier thinning and steepening,

Table 8. Glacier change, 1988 to 2009. Note that there is particularly limited data for 1997. Uncertainty margin for 2009 includes uncertainties inherent in polygon determination. As the analysis of frontal change in 2001 and 1988 assumes no migration of ice divides, uncertainty is calculated by using a 3-pixel wide buffer on either side of the ice front only and is, therefore, a minimum uncertainty of only the ice front change. Where data is missing, it is assumed that the glacier did not change in size between that year and the last year for which data was available; therefore, these figures are a minimum estimate. TP=Trinity Peninsula. JRI=James Ross Island. VI=Vega Island. IIC=Island Ice Caps. All=all glaciers. All area is given in km².

| Area | Area 2009 | Area 2001 | Area 1997 | Area 1988 |
|-----------|----------------|---------------|-----------|--------------|
| All | 8140.4 ± 261.7 | 8414 ± 49.1 | 8532.1 | 9460 ± 395.6 |
| TP | 5827.3 ± 153.9 | 5961.6 ± 28.4 | 5980.3 | 6689 ± 218.1 |
| JRI | 1780.5 ± 86.2 | 1902.4 ± 15.2 | 1992.6 | 2192 ± 136.1 |
| VI | 167.8 ± 14.8 | 169.8 ± 1.2 | 169.8 | 178 ± 19.3 |
| IIC | 364.7 ± 6.8 | 380.6 ± 4.8 | 389.5 | 400 ± 22.2 |
| Area Lost | 2001–2009 | 1988–2001 | 1997–2001 | 1988–2009 |
| All | 274.1 | 1045.5 | 117.7 | 1319.5 |
| TP | 134.3 | 727.8 | 18.7 | 862.0 |
| JRI | 121.9 | 290.0 | 90.2 | 411.9 |
| VI | 1.9 | 8.1 | 0.00 | 10.0 |
| IIC | 16.0 | 19.6 | 0.00 | 35.6 |
| Area Gain | 2001–2009 | 1988–2001 | 1988–2009 | |
| All | 0.09 | 0.08 | 0.13 | |
| TP | 0.00 | 0.03 | 0.03 | |
| JRI | 0.06 | 0.05 | 0.10 | |
| VI | 0.00 | 0.00 | 0.00 | |
| IIC | 0.00 | 0.00 | 0.00 | |

further exacerbating increased calving rates for tidewater glaciers (Meier and Post, 1987; van der Veen, 2002) and possibly contributing to short-term small glacier advances.

6.2 Impact of the disintegration of Prince Gustav Ice Shelf

The remnant of PGIS in Röhss Bay on James Ross Island (Fig. 1) dramatically disintegrated after 2001. Small ice shelves are susceptible to small changes in temperature and mass balance of tributary glaciers (Glasser et al., 2011). The retreat of ice shelves from pinning points (such as Persson Island) can result in enhanced calving and rapid retreat. The acceleration of recession of the ice shelf in Röhss Bay after 2001 was, therefore, caused by recession from the pinning point, exacerbated by continued atmospheric warming. Small amounts of growth in some ice-shelf glaciers was observed from 1988 to 2001. However, this advance was subsumed by overall glacier shrinkage (cf. Fig. 7). In addition, up-glacier thinning may result in steepening, increased driving stress, faster flow and short-term advance (cf. Meier and Post, 1987).

The shrinkage of marine-terminating glaciers in the northern Antarctic Peninsula highlights some important trends. For glaciers feeding PGIS, rates of shrinkage were highest following ice-shelf disintegration. Ice-shelf removal can lead to the destabilisation of tributary glaciers, as ice shelves re-

duce longitudinal stresses and limit glacier motion upstream of the ice shelf (Pritchard and Vaughan, 2007; Hulbe et al., 2008). These tributary glaciers began to stabilise and reach a new dynamic equilibrium after 2001 and rates of recession began to reduce once they become stabilised in their narrow fjords. Indeed, fjord geometry has previously been observed to be a major control on tidewater glacier advance and recession rates (Meier and Post, 1987), with shrinkage slowing as a result of enhanced backstress and pinning against the fjord sides. After 2001, the region, therefore, entered a period of “normal” glacier shrinkage. The northern Antarctic Peninsula region has, thus, had three distinctive phases: 1988–1995, the stable ice-shelf period; 1995–2001, the period of ice-shelf disintegration and rapid readjustment of the ice-shelf tributary glaciers to new boundary conditions; and 2001–2009, when all glaciers are shrinking in response to changes in atmospheric and oceanic temperatures. Structural glaciological controls are also strongly influencing patterns and rates of retreat of floating tongues following ice-shelf disintegration.

Previous workers have hypothesised that the disintegration of the ice shelf may have affected the regional climate (Rau et al., 2004). The response of land-terminating glaciers is particularly interesting, because these glaciers exhibited their highest annual rates of retreat in the ice-shelf disintegration period. Land-terminating glaciers are directly influenced by climatic perturbations and their mass balances are, therefore,

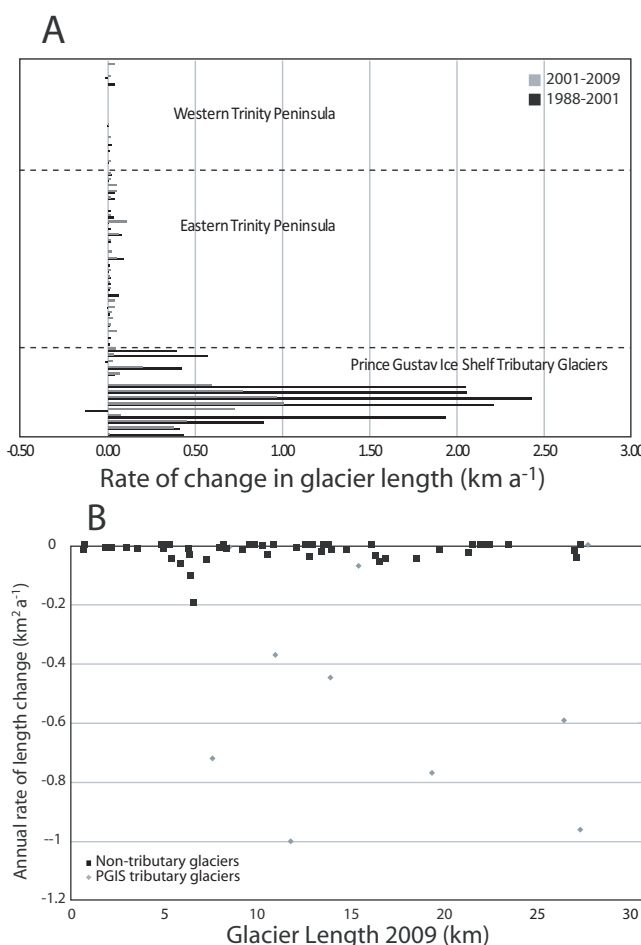


Fig. 6. Tidewater glacier length. **(A)** Rates of glacier length change in tidewater glaciers on Trinity Peninsula. **(B)** Scatter plot showing poor correlation between 2009 glacier length and length changes.

a sensitive indicator of climate variability (Oerlemans, 2005). In addition, small glaciers on James Ross Island may be particularly susceptible to changes in local climate because of the large land area, which has a low albedo. It has been suggested that ice-shelf break up would immediately affect the climate system through the formation of deep water (Hulbe et al., 2004). The removal of the ice shelf would have raised local air temperatures through the availability of more ice-free water in summer.

6.3 Glacier hypsometry and future changes in equilibrium line altitude

The more stable glaciers on the western Peninsula typically have equi-dimensional or top-heavy hypsometric curves (Figs. 3, 4), which, combined with high snowfalls (van Lipzig et al., 2004), render them less susceptible to the changes in ELA brought about by changing atmospheric temperatures (cf. Jiskoot et al., 2009). These glaciers have large accumulation areas situated at high altitudes, which con-

tributes to their stability. The hypsometric curves of these grounded tidewater glaciers indicate that they will retain large accumulation areas if future recession occurs and, thus, shrinkage will be slow, rendering them less sensitive to an upwards shift in the ELA.

Given an adiabatic lapse rate of -5.8°C per 1000 m (Aristarain et al., 1987), an increase of 2°C would raise ELAs over the northern Antarctic Peninsula by 345 m. This is illustrated as ELA_{2C} on the hypsometric curves in Fig. 4, and it is immediately obvious that the differential hypsometry of the glaciers may be a significant control on rates of recession in the future. Bottom-heavy glaciers with low-lying ELAMEAN values (such as GAP12) and top-heavy glaciers with high ELAMEAN values (such as GAP13; Fig. 4) are most sensitive to change. In general, however, the tidewater glaciers on eastern Trinity Peninsula have large, high-elevation accumulation areas. Without a further strong perturbation to the prevailing climate, these large tidewater glaciers will most likely stabilise when they reach their grounding-lines. The ELA_{2C} calculated for these glaciers indicates that even with a 2°C rise in temperature, glaciers will still retain accumulation areas covering at least 40 % of the glacier surface, assuming that glacier hypsometries remain similar. The steady steep slopes on these glaciers also render them less vulnerable; a rise in ELA does not expose a significantly larger area to ablation. Additionally, as these glaciers retreat towards the grounding-line zones, ablation areas will decrease in size, resulting in the glaciers reaching a steady state.

The outlet glaciers draining Mount Haddington Ice Cap typically have a large, low-angled upland accumulation area on the ice cap, a steep icefall over cirque headwalls, and a very flat and low-lying partly floating or floating tongue. The large flat accumulation area renders the glacier susceptible to rapid loss of accumulation area in the event of a rise in ELA. These attributes can be observed in the stepped hypsometric curves of GIJR123 and GIJR115 (Fig. 3g). Rising sea levels would encourage further grounding-line retreat. GIJR27, for example, may be particularly vulnerable as this tidewater glacier has a large, low-lying flat tongue and ELA_{2C} plots above the accumulation area. Other glaciers with low-lying tongues will have projected accumulation areas covering only 20–30 % of their area (e.g., GIJR72, GIJR115, GIJR128, GIJR136). These glaciers are likely to continue to retreat very rapidly.

7 Conclusions

In this paper, we have described changes in all glaciers in the Trinity Peninsula region. We provide the first detailed inventory of 194 glaciers on Trinity Peninsula and islands to the southeast, with detailed estimates of size, length, elevation ranges, ELA, slope, aspect, hypsometry, morphological descriptors, form and classification. These data will be useful

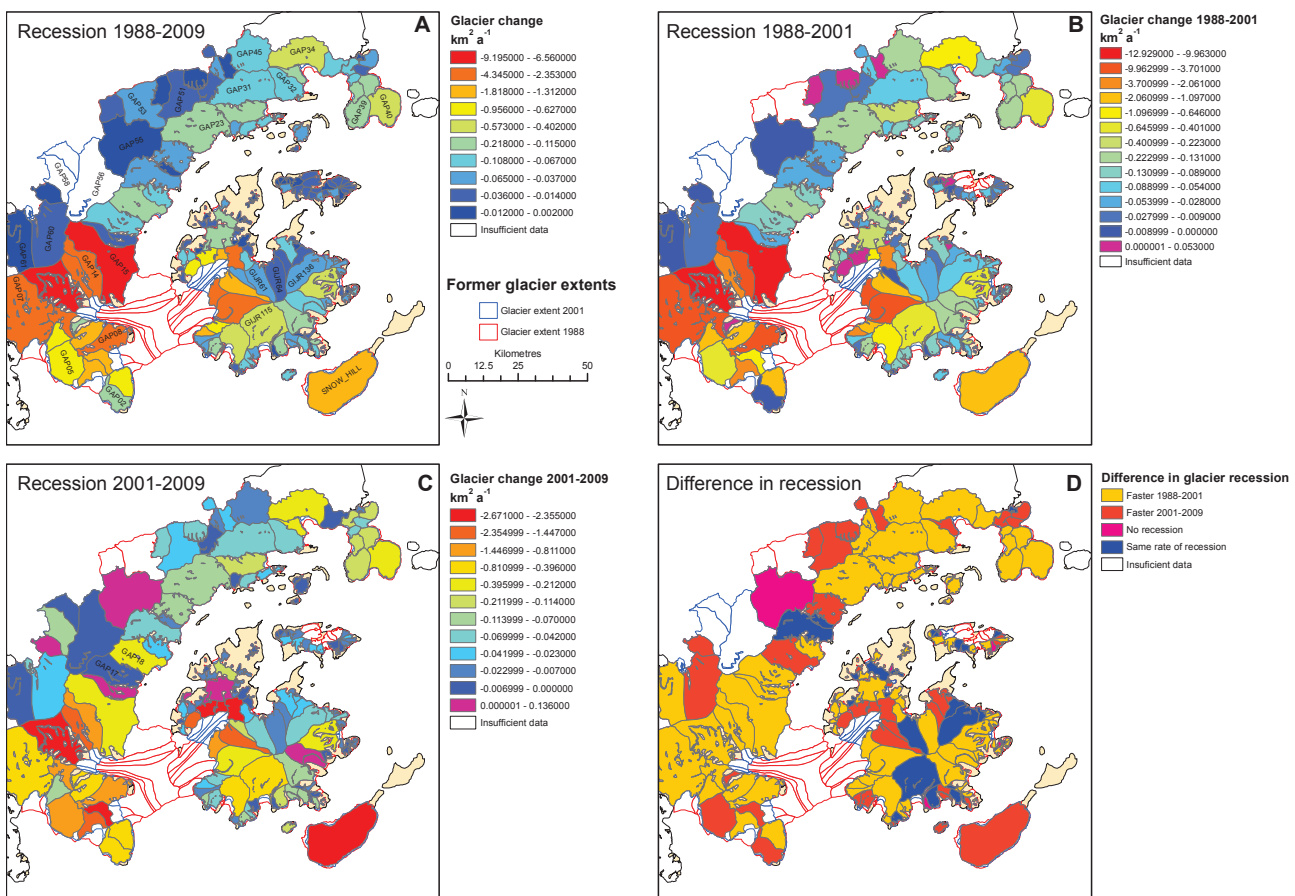


Fig. 7. Annual rates of shrinkage for different time periods. Glaciers in red shrank fastest. Glaciers in purple advanced. **(A)** Overall shrinkage, 1988–2009. Note the slow rates of shrinkage on western Trinity Peninsula. **(B)** Rates of shrinkage, 1988–2001. PGIS tributary glaciers shrank fastest. Note that two PGIS-tributary glaciers in Röhss Bay advanced during this period. **(C)** Rates of shrinkage, 2001–2009. Note a few small advancing glaciers. **(D)** Difference in shrinkage rates. Glaciers in blue shrank fastest between 1988 and 2001; glaciers in red shrank fastest after 2001. Note that PGIS tributary glaciers shrank slower after 2001.

to researchers seeking to predict the future behaviour of this climatically sensitive region.

We measured variability in glacier length and area changes on the northern Antarctic Peninsula between 1988, 1997, 2001 and 2009. Changes in glacier area and length presented in this study considerably extend the hitherto available geographical coverage and amount of detail available for understanding the impacts of climate change on the cryosphere.

Of the 194 glaciers surveyed, 90 % showed rapid areal decline from 1988–2001 and 79 % retreated from 2001–2009, although the rates and patterns of change vary substantially. Overall, annual rates of shrinkage were higher from 1988–2001 in tidewater and ice-shelf tributary glaciers. Some glaciers on western Trinity Peninsula, glaciers in Röhss Bay on James Ross Island and Snow Hill Island shrank faster from 2001–2009. Annual rates of area loss in land-terminating glaciers were also higher from 1988–2001. Three distinct phases were observed: 1988–1997 (the ice-shelf and ice-shelf disintegration era); 1997–2001 (period of

immediate adjustment); 2001–2009 (period of stabilisation and long-term adjustment to new dynamic equilibrium and general climate-driven recession). The total glacierised area in the northern Antarctic Peninsula has declined at an average of $30.4 \pm 0.99 \text{ km}^2 \text{a}^{-1}$ since 2001, with total losses of glacierised area of 11.1 % from 1988–2001 and 3.3 % from 2001–2009.

Tidewater glaciers on western Trinity Peninsula remained stable between 1988 and 2009, and to date show only slow rates of shrinkage. They receive abundant snow from prevailing south-westerly winds and, unless strong perturbation to this system occurs, will probably remain stable in areal extent. This inference does not take account of glacier thinning, which is observed in other parts of the Antarctic Peninsula, even after frontal stabilisation has occurred (Rott et al., 2011). In contrast, tidewater glaciers on eastern Trinity Peninsula shrank more than glaciers on western Trinity Peninsula, but recession will slow in the future as they retreat towards their grounding zones. This differing regional

response can probably be attributed to precipitation gradients, exacerbated by climatic warming and differential wind patterns (cf. van Lipzig et al., 2004; Aristarain et al., 1987; Vaughan et al., 2003).

On James Ross Island, the largest areal changes have been from low-lying tidewater glaciers. Rates of change for tidewater glaciers are likely to continue in response to continued atmospheric warming. The primary control for the widespread glacier retreat in northeast Antarctic Peninsula is apparently the observed climatic warming, with glacier size, length, slope, type, ELA and altitude exerting a strong mitigating or enhancing role.

Despite fears of continued run-away retreat and terminal destabilisation of tidewater glaciers, this study shows that ice-shelf tributary glaciers are more likely to undergo a time-limited period of adjustment. Ultimately, ice-shelf tributary glaciers will find a new dynamic equilibrium, and then retreat slowly in response to warming climates and rising ELAs. We, therefore, anticipate that the results of this project will have significant relevance to studies concerned with the more southerly ice shelves that surround the Antarctic Peninsula. The behaviour of PGIS tributary glaciers and their long-term response to ice-shelf removal can be used to model and predict glacier response to contemporary and future ice-shelf disintegration events.

Supplementary material related to this article is available online at: <http://www.the-cryosphere.net/6/1031/2012/tc-6-1031-2012-supplement.zip>.

Acknowledgements. This work was funded by NERC grant AFI 9-01 (NE/F012942/1). It is a contribution to the SCAR ACE (Antarctic Climate Evolution) Programme. The authors are grateful for helpful and constructive criticism and comments from Hester Jiskoot, Matt King, Tobias Bolch, Mauri Pelto, S. Marinsek and an anonymous referee. The authors acknowledge Etienne Berthier and the Centre National d'Etudes Spatiales (CNES) for the SPOT-5 images and the SPIRIT DEM. Neil Glasser was provided with ASTER images as a NASA-supported researcher. The 1997 glacier frontal positions were determined from the Coastal Change shapefiles (<http://www.add.scar.org>), mapped by Cook et al. (2005). Stefan Senk and Tristram Irvine-Fynne are acknowledged for their help in programming and statistics.

Edited by: G. H. Gudmundsson

References

- Aristarain, A. J., Pinglot, J. F., and Pourchet, M.: Accumulation and temperature measurements on the James Ross Island ice cap, Antarctic Peninsula, Antarctica, *J. Glaciol.*, 33, 357–362, 1987.
- Benn, D. I., Hulton, N. R. J., and Mottram, R. H.: “Calving laws”, “sliding laws” and the stability of tidewater glaciers, *Ann. Glaciol.*, 46, 123–130, 2007.
- Bolch, T., Menounos, B., and Wheate, R.: Landsat-based inventory of glaciers in western Canada, 1985–2005, *Remote Sens. Environ.*, 114, 127–137, 2010.
- Braithwaite, R. J. and Raper, S. C. B.: Estimating equilibrium-line altitude (ELA) from glacier inventory data, *Ann. Glaciol.*, 50, 127–132, 2009.
- British Antarctic Survey: Antarctic Sound and James Ross Island, Northern Antarctic Peninsula, Series BAS (UKAHT) Sheets 3A and 3B, 1, Cambridge, 2010.
- Carrivick, J. L. and Brewer, T. R.: Improving local estimations and regional trends of glacier equilibrium line altitudes, *Geogr. Ann. A*, 86, 67–79, 2004.
- Cook, A. J., Fox, A. J., Vaughan, D. G., and Ferrigno, J. G.: Retreating glacier fronts on the Antarctic Peninsula over the past half-century, *Science*, 308, 541–544, 2005.
- Cook, A. J. and Vaughan, D. G.: Overview of areal changes of the ice shelves on the Antarctic Peninsula over the past 50 years, *The Cryosphere*, 4, 77–98, doi:10.5194/tc-4-77-2010, 2010.
- De Angelis, H. and Skvarca, P.: Glacier surge after ice shelf collapse, *Science*, 299, 1560–1562, 2003.
- Evans, I. S.: Local aspect asymmetry of mountain glaciers: a global survey of consistency of favoured directions of glacier numbers and altitudes, *Geomorphology*, 73, 166–184, 2006.
- Ferrigno, J. G., Cook, A. J., Foley, K. M., Williams, R. S., Swiethinbank, C., Fox, A. J., Thomson, J. W., and Sievers, J.: Coastal-Change and Glaciological Map of the Trinity Peninsula Area and South Shetland Islands, USGS, Antarctica, 1843–2001, 32 pp., 2006.
- Fricker, H. A., Coleman, R., Padman, L., Scambos, T. A., Bohlander, J., and Brunt, K. M.: Mapping the grounding zone of the Amery Ice Shelf, East Antarctica using InSAR, MODIS and ICESat, *Antarct. Sci.*, 21, 515–532, 2009.
- Gille, S. T.: Decadal-scale temperature trends in the Southern Hemisphere Ocean, *J. Climatol.*, 21, 4749–4765, 2008.
- Glasser, N. F., Kulessa, B., Luckman, A., Jansen, D., King, E. C., Sammonds, P. R., Scambos, T. A., and Jezek, K. C.: Surface structure and stability of the Larsen C Ice Shelf, Antarctic Peninsula, *J. Glaciol.*, 55, 400–410, 2009.
- Glasser, N. F., Scambos, T. A., Bohlander, J. A., Truffer, M., Pettit, E. C., and Davies, B. J.: From ice-shelf tributary to tidewater glacier: continued rapid glacier recession, acceleration and thinning of Röhss Glacier following the 1995 collapse of the Prince Gustav Ice Shelf on the Antarctic Peninsula, *J. Glaciol.*, 57, 397–406, 2011.
- Haeberli, W. and Hoelzle, M.: Application of inventory data for estimating characteristics of and regional climate-change effects on mountain glaciers: a pilot study with the European Alps, *Ann. Glaciol.*, 21, 206–212, 1995.
- Holland, P. R., Jenkins, A., and Holland, D. M.: Ice and ocean processes in the Bellingshausen Sea, Antarctica, *J. Geophys. Res.*, 115, C05020, doi:10.1029/2008JC005219, 2010.
- Hulbe, C. L., MacAyeal, D. R., Denton, G. H., Kleman, J., and Lowell, T. V.: Catastrophic ice shelf break up as the source of Heinrich Event icebergs, *Paleoceanography*, 19, PA1004, doi:10.1029/2003PA000890, 2004.
- Hulbe, C. L., Scambos, T. A., Youngberg, T., and Lamb, A. K.: Patterns of glacier response to disintegration of the Larsen B ice shelf, Antarctic Peninsula, *Glob. Planet. Change*, 63, 1–8, 2008.

- Ivins, E. R., Watkins, M. M., Tuan, D.-N., Dietrich, R., Casassa, G., and Rülke, A.: On-land ice loss and glacial isostatic adjustment at the Drake Passage: 2003–2009, *J. Geophys. Res.*, 116, 22 pp., 2011.
- Jiskoot, H., Curran, C. J., Tessler, D. L., and Shenton, L. R.: Changes in Clemenceau Icefield and Chaba Group glaciers, Canada, related to hypsometry, tributary detachment, length-slope and area-aspect relations, *Ann. Glaciol.*, 50, 133–143, 2009.
- King, J. C., Turner, J., Marshall, G. J., Connelly, W. M., and Lachlan-Cope, T. A.: Antarctic Peninsula climate variability and its causes as revealed by analysis of instrumental records, in: Antarctic Peninsula climate variability: historical and palaeoenvironmental perspectives, edited by: Domack, E. W., Leventer, A., Burnett, A., Bindschadler, R., Convey, P., and Kirby, M., Washington DC, American Geophysical Union, Antar. Res. S., 17–30, 2003.
- Korona, J., Berthier, E., Bernard, M., Remy, F., and Thouvenot, E.: SPIRIT. SPOT 5 stereoscopic survey of Polar Ice: Reference Images and Topographies during the fourth International Polar Year (2007–2009), ISPRS, *J. Photogram. Remote Sens.*, 64, 204–212, 2009.
- Lambrecht, A., Sandhager, H., Vaughan, D. G., and Mayer, C.: New ice thickness maps of Filchner-Ronne Ice Shelf, Antarctica, with specific focus on grounding lines and marine ice, *Antarct. Sci.*, 19, 521–532, 2007.
- Leclercq, P. W., Oerlemans, J., and Cogley, J. G.: Estimating the glacier contribution to sea-level rise for the period 1800–2005, *Survey Geophysics*, 1–17, doi:10.1007/s10712-011-9121-7, 2011.
- Leonard, K. C. and Fountain, A. G.: Map-based methods for estimating glacier equilibrium-line altitudes, *J. Glaciol.*, 49, 329–336, 2003.
- Lopez, P., Chevallier, P., Favier, V., Pouyaud, B., Ordenes, F., and Oerlemans, J.: A regional view of fluctuations in glacier length in southern South America, *Global Planet. Change*, 71, 85–108, 2010.
- Mayewski, P. A., Meredith, M. P., Summerhayes, C. P., Turner, J., Worby, A., Barrett, P. J., Casassa, G., Bertler, N. A. N., Bracegirdle, T., Naveira Garabato, A. C., Bromwich, D., Campell, H., Hamilton, G. S., Lyons, W. B., Maasch, K. A., Aoki, S., Xiao, C., and van Ommen, T.: State of the Antarctic and Southern Ocean climate system, *Reviews of Geophysics*, 47, 1–38, 2009.
- Meier, M. F. and Post, A.: Fast tidewater glaciers, *J. Geophys. Res.*, 92, 9051–9058, 1987.
- Meredith, M. P. and King, J. C.: Rapid climate change in the ocean west of the Antarctic Peninsula during the second half of the 20th Century, *Geophys. Res. Lett.*, 32, 1–5, 2005.
- Morris, E. M. and Vaughan, A. P. M.: Spatial and temporal variation of surface temperature on the Antarctic Peninsula and the limit of viability of ice shelves, in: Antarctic Peninsula climate variability: historical and palaeoenvironmental perspectives, edited by: Domack, E. W., Leventer, A., Burnett, A., Bindschadler, R., Convey, P., and Kirby, M., Washington DC, American Geophysical Union, Antar. Res. S., 79, 61–68, 2003.
- Oerlemans, J.: Extracting a climate signal from 169 glacier records, *Science*, 308, 675–677, 2005.
- Paul, F. and Svoboda, F.: A new glacier inventory on southern Baffin Island, Canada, from ASTER data: II. Data analysis, glacier change and applications, *Ann. Glaciol.*, 50, 22–31, 2009.
- Paul, F., Barry, R. G., Cogley, J. G., Frey, H., Haeberli, W., Ohmura, A., Ommanney, C. S. L., Raup, B., Rivera, A., and Zemp, M.: Guidelines for the compilation of glacier inventory data from digital sources, GLIMS, Global Land Ice Measurement from Space, NSIDC, 23 pp., 2010.
- Powell, R. D.: Grounding-line systems as second-order controls on fluctuations of tidewater termini of temperate glaciers, in: *Glacial marine sedimentation; palaeoclimatic significance*, edited by: Anderson, J. B. and Ashley, G. M., Boulder, Colorado, *Geol. S. Am. S.*, 261, 75–94, 1991.
- Pritchard, H. D. and Vaughan, D. G.: Widespread acceleration of tidewater glaciers on the Antarctic Peninsula, *J. Geophys. Res.-Earth*, 112, 1–10, 2007.
- Rabassa, J., Skvarca, P., Bertani, L., and Mazzoni, E.: Glacier inventory of James Ross and Vega Islands, Antarctic Peninsula, *Ann. Glaciol.*, 3, 260–264, 1982.
- Racoviteanu, A. E., Paul, F., Raup, B., Khalsa, S. J. S., and Armstrong, R.: Challenges and recommendations in mapping of glacier parameters from space: results of the 2008 Global Land Ice Measurements from Space (GLIMS) workshop, Boulder, Colorado, USA, *Ann. Glaciol.*, 50, 53–69, 2009.
- Raper, S. C. B. and Braithwaite, R. J.: Glacier volume response time and its links to climate and topography, *The Cryosphere*, 3, 183–194, 2009, <http://www.the-cryosphere-discuss.net/3/183/2009/>.
- Rau, F., Mauz, F., de Angelis, H., Ricardo, J., Neto, J. A., Skvarca, P., Vogt, S., Saurer, H., and Gossmann, H.: Variations of glacier frontal positions on the northern Antarctic Peninsula, *Ann. Glaciol.*, 39, 525–530, 2004.
- Rau, F., Mauz, F., Vogt, S., Khalsa, S. J. S., and Raup, B.: Illustrated GLIMS Glacier Classification Manual, Version 1.0. GLIMS Regional Centre, “Antarctic Peninsula”, GLIMS (Global Land Ice Measurement from Space), NSIDC, 36 pp., 2005.
- Raup, B. and Khalsa, S. J. S.: GLIMS Analysis Tutorial, www.GLIMS.org, GLIMS, Global Land Ice Measurements from Space, NSIDC, 15 pp., 2010.
- Raup, B., Kääb, A., Kargel, J. S., Bishop, M. P., Hamilton, G., Lee, E., Paul, F., Rau, F., Soltesz, D., Khalsa, S. J. S., Beedle, M., and Helm, C.: Remote sensing and GIS technology in the Global Land Ice Measurements from Space (GLIMS) Project, *Comput. Geosci.*, 33, 104–125, 2007a.
- Raup, B., Racoviteanu, A., Khalsa, S. J. S., Helm, C., Armstrong, R., and Arnaud, Y.: The GLIMS geospatial glacier database: A new tool for studying glacier change, *Global Planet. Change*, 56, 101–110, 2007b.
- Reinartz, P., Müller, R., Lehner, M., and Schroeder, M.: Accuracy analysis for DEM and orthoimages derived from SPOT HRS stereo data using direct georeferencing, ISPRS, *J. Photogram.*, 60, 160–169, 2006.
- Rott, H., Skvarca, P., and Nagler, T.: Rapid collapse of northern Larsen Ice Shelf, Antarctica, *Science*, 271, 788–792, 1996.
- Scambos, T., Hulbe, C., and Fahnestock, M.: Climate-induced ice shelf disintegration in the Antarctic Peninsula, in: *Antarctic Peninsula Climate Variability*, edited by: Domack, E. W., Leventer, A., Burnett, A., Bindschadler, R., Convey, P., and Kirby, M., Antar. Res. S., 79, 79–92, 2003.
- Scambos, T. A., Bohlander, J. A., Shuman, C. A., and Skvarca, P.: Glacier acceleration and thinning after ice shelf collapse in

- the Larsen B embayment, Antarctica, *Geophys. Res. Lett.*, 31, L18402, doi:10.1029/2004GL020670, 2004.
- Skvarca, P. and De Angelis, H.: Impact assessment of regional climatic warming on glaciers and ice shelves of the northeastern Antarctic Peninsula, in: Antarctic Peninsula climate variability: historical and palaeoenvironmental perspectives, edited by: Domack, E. W., Levener, A., Burnett, A., Bindshadler, R., Convey, P., and Kirby, M., *Antar. Res. S.*, 79, 69–78, 2003.
- Skvarca, P., Rott, H., and Nagler, T.: Satellite imagery, a base line for glacier variation study on James Ross Island, Antarctica, *Ann. Glaciol.*, 21, 291–296, 1995.
- Skvarca, P., De Angelis, H., and Ermolin, E.: Mass balance of “Glaciar Bahia del Diablo”, Vega Island, Antarctic Peninsula, *Ann. Glaciol.*, 39, 209–213, 2004.
- Smellie, J. L., Johnson, J. S., McIntosh, W. C., Esser, R., Gudmundsson, M. T., Hambrey, M. J., and van Wyk de Vries, B.: Six million years of glacial history recorded in volcanic lithofacies of the James Ross Island Volcanic Group, Antarctic Peninsula, *Palaeogeogr. Palaeocl.*, 260, 122–148, 2008.
- Svoboda, F. and Paul, F.: A new glacier inventory on southern Baffin Island, Canada, from ASTER data: I. Applied methods, challenges and solutions, *Ann. Glaciol.*, 50, 11–21, 2009.
- Torsnes, I., Rye, N., and Nesje, A.: Modern and Little Ice Age Equilibrium-Line Altitudes on outlet valley glaciers from Jostedalsbreen, Western Norway: an evaluation of different approaches to their calculation, *Arctic Alpine Res.*, 25, 106–116, 1993.
- Turner, J., Colwell, S. R., Marshall, G. J., Lachlan-Cope, T. A., Carelton, A. M., Jones, P. D., Lagun, V., Reid, P. A., and Iagovkina, S.: Antarctic climate change during the last 50 years, *Int. J. Climatol.*, 25, 279–294, 2005.
- van den Broeke, M. R. and van Lipzig, N. P. M.: Changes in Antarctic temperature, wind and precipitation in response to the Antarctic Oscillation, *Ann. Glaciol.*, 39, 119–126, 2004.
- van der Veen, C. J.: Calving glaciers, *Prog. Phys. Geog.*, 26, 96–122, 2002.
- van Lipzig, N. P. M., King, J. C., Lachlan-Cope, T., and van den Broeke, M.: Precipitation, sublimation and snow drift in the Antarctic Peninsula region from a regional atmospheric model, *J. Geophys. Res.*, 109, D24106, doi:10.1029/2004JD004701, 2004.
- Vaughan, D. G., Marshall, G. J., Connally, W. M., Parkinson, C., Mulvaney, R., Hodgson, D. A., King, J. C., Pudsey, C. J., and Turner, J.: Recent rapid regional climate warming on the Antarctic Peninsula, *Climatic Change*, 60, 243–274, 2003.